Dislocation structure for one-dimensional strain in a shocked crystal

F. A. Bandak
Naval Surface Warfare Center, White Oak Laboratory, Silver Spring, Maryland 20903
and The Johns Hopkins University, Baltimore, Maryland 21218

R. W. Armstrong
University of Maryland, College Park, Maryland 20742

A. S. Douglas
The Johns Hopkins University, Baltimore, Maryland 21218
(Received 26 December 1991)

Dislocation structures proposed to model plastic deformation at a shock front are analyzed. The creation and glide movement of the dislocations are considered. Glide-type movement violates the condition of one-dimensional strain except if dislocation dipoles with Burgers vectors parallel and antiparallel to the shock propagation direction are directly generated by alternating shear stresses as in a punching action. The stress, strain, and dilatation characteristics are presented for a dislocation structure proposed by Armstrong, Miller, and Sandusky (AMS) to give a residual one-dimensional strain state. The AMS dislocation structure is related to independent results from a molecular-dynamics description of shear displacements in a shocked triangular lattice and is used as a basis for estimating the extent of postshock strengthening levels. The shock-strengthening predictions are in reasonable agreement with postshock deformation measurements.

I. INTRODUCTION

In a dislocation-model description of a plane shock front, Smith[1] proposed that a cross grid of edge dislocations with net Burgers vectors in the front was distributed across the planar interface to account for the proposed mismatch of lattice planes occurring between shock-compressed and unshocked material. Meyers[2] extended the model to consider the possibility that the mismatch dislocations would occur in periodic zones approximately parallel to the shock front. Following Smith,[1] Meyers put the cross-grid dislocations onto shear planes oriented at 45° to the front, thereby indicating that the local lattice mismatch could be accommodated by shear deformation.[2] The resulting dislocation structure of the Meyers model is shown in Fig. 1(a). Realistic dislocation densities were estimated for the model.

A second dislocation model has been proposed by Armstrong, Miller, and Sandusky,[3] hereafter labeled AMS, as shown in Fig. 1(b). In this case, elementary shear zones are imagined to emanate from points along the shock front and to be distributed in an interlocked manner such that the displaced dislocations react to form prismatic edge dislocation dipoles with Burgers vectors parallel, not perpendicular, to the direction of shock wave propagation [Fig. 1(c)]. The reacted dislocations produce a residual internal state of essentially one-dimensional strain, as employed in the ideal characterization of a plane shock front.

The two dislocation models described above are proposed for events that occur in a time period of highly transient strain phenomena. The models illustrate frozen views of possible dislocation processes occurring under maximum shock compression conditions. Evidence that fundamental questions remain to be resolved about dislocation processes in shocks is provided by Johnson's[4] concern regarding the net sign of dislocations needed to accomplish the shock-generated shearing process at the initial impact surface of a crystal. The AMS model has the particular reaction feature of satisfying a final condition of one-dimensional strain while not producing a net sign for the total dislocation distribution. Equal numbers of positive and negative dislocations occur in a particular arrangement that promotes the survival of a residual dislocation nanoscale structure in the unloaded material. This nanometer-scale defect substructure is of interest for its relation to molecular-dynamics modeling of shock-defect interactions[5–7] and to the subsequent strength properties of shocked materials. Our purpose here is to assess these dislocation models in terms of their limited ability to satisfy the accepted plane shock assumption of a one-dimensional strain state and to relate the AMS model to measurements of postshock strengthening.

II. STRESS OR STRAIN STATE CONSIDERATIONS

Plane shock wave compression is taken to produce unidirectional deformation in the direction of wave propagation for an assumed isotropic crystal. The associated strain tensor has only one nonvanishing component ϵ_{22}. This is defined as

$$\epsilon_{22}=(V-V_0)/V_0 , \tag{1}$$

where V_0 and V are the uncompressed and compressed volumes, respectively. The zero transverse strains in Hooke's isotropic relations, for example, involving the

strain in one transverse direction,

$$\epsilon_{11}=(1/E)[\sigma_{11}-\nu(\sigma_{22}+\sigma_{33})]=0\ , \tag{2}$$

lead to the associated stress state

$$[\sigma]=\frac{E(V-V_0)}{V_0(1+\nu)(1-2\nu)}\begin{bmatrix}\nu & 0 & 0\\ 0 & 1-\nu & 0\\ 0 & 0 & \nu\end{bmatrix}\ , \tag{3}$$

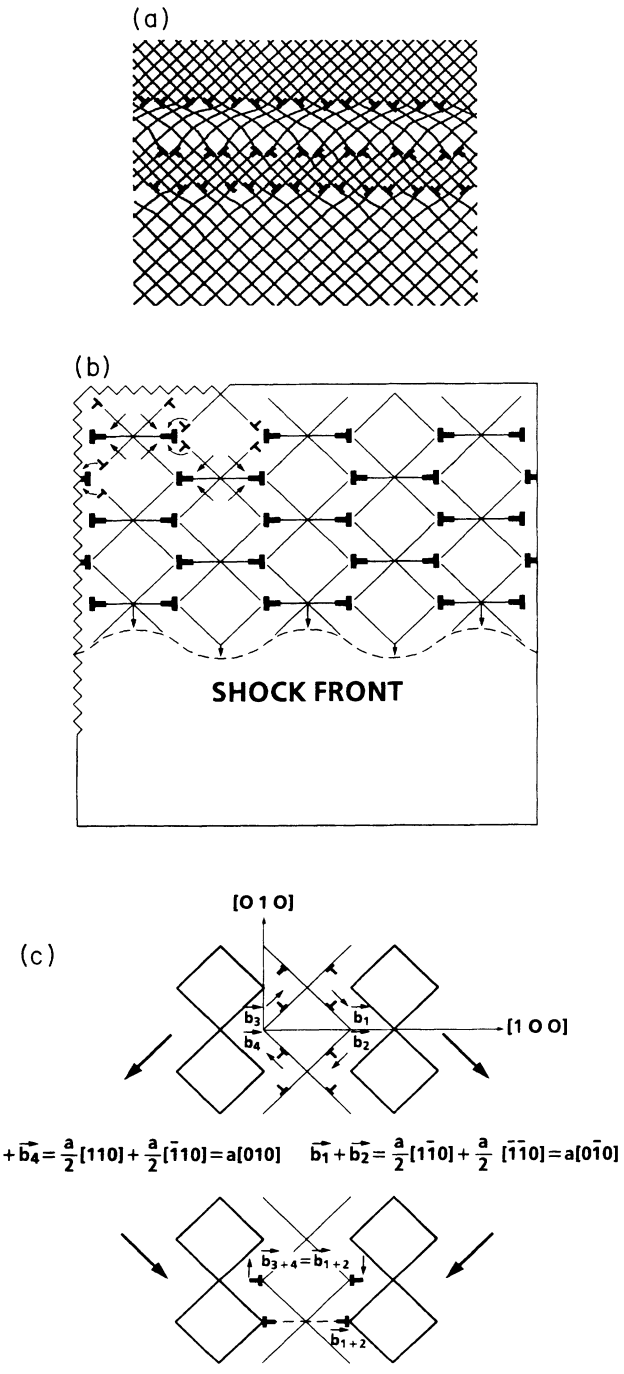

FIG. 1. (a) Dislocation structure of the Meyers model (Ref. 2). (b) Dislocation dipole structure of the Armstrong-Miller-Sandusky model (Ref. 3). (c) Specific reactions for dipole formation.

where E is the elastic modulus and ν is Poisson's ratio.

This stress state is considered here for the simple case where dislocations can move on planes coincident with planes of maximum shear stress, namely those oriented at 45° to the straining direction. The maximum shear stress $\tau_{\max}$ given as

$$\tau_{\max}=(\sigma_{22}-\sigma_{11})/2\ , \tag{4}$$

with Eq. (3) becomes

$$\tau_{\max}=\frac{1-2\nu}{2(1-\nu)}\sigma_{22}=\frac{E(V-V_0)}{2V_0(1+\nu)}\ . \tag{5}$$

This maximum shear stress condition should, in a homogeneous sense, exist across the shock front on every plane oriented at 45° relative to the loading direction. The value of the imposed strain and its rate of propagation lead to the expectation that dislocation generation and movement should occur at numerous local points on the front rather than at more remote locations. The large strains must correspondingly be relaxed locally.

A uniform distribution of heterogeneities on the scale of point defects provides the possibility that a nearly uniform distribution of dislocations might occur under shock conditions. These defects would locally lower the value of the compression stress σ_{22} required to achieve $\tau_{\max}$ for the generation of dislocations, even on the scale of a single atomic vacancy. A molecular-dynamics simulation has been described for the generation of dislocations from a rather large ten-vacancy cluster under plane shock compression.[7] Figure 2 shows the pre- and

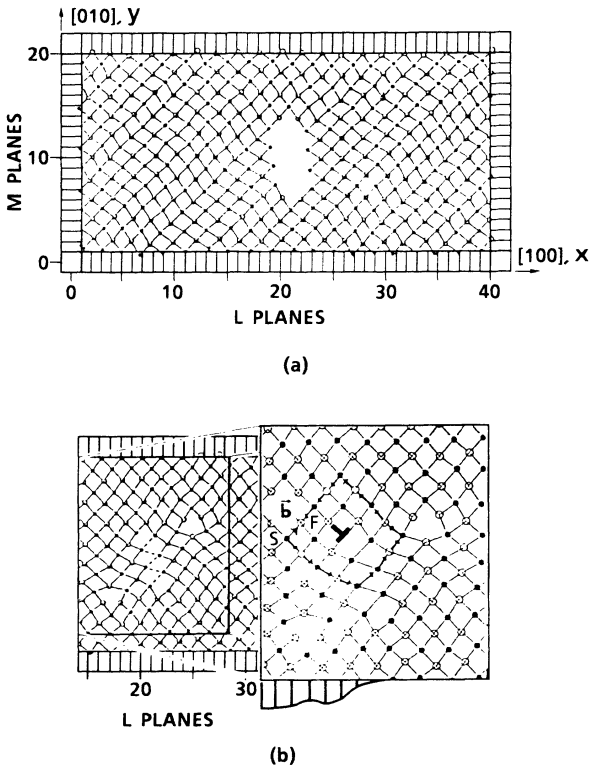

FIG. 2. Molecular-dynamics computations of (a) preshock vacancy cluster leading to (b) postshock dislocation dipole structure.

postshock compression configurations of the cluster.

The theoretical shear stress τ_h at which dislocations might be homogeneously generated in shocked nickel has been estimated by Meyers.[2] On that basis, dislocation densities were determined for various (V/V_0) values without regard for the lateral strains produced by the glide-type dislocation displacements. Such displacements have to produce axial and lateral strains under any type of compression. This occurs for each of the models described, although the reacted dislocation arrangement in the AMS model does produce a residual state of one-dimensional strain.

III. DISLOCATION MOVEMENT STRAIN

To calculate the strain resulting from the movement of the AMS dislocations prior to reaction, we consider the single intersecting shear element of Fig. 3 as taken from the system in Fig. 1(c). The simple shear glide in the x_1' direction, along a glide plane with a normal in the x_2' direction, produces displacements that can be represented

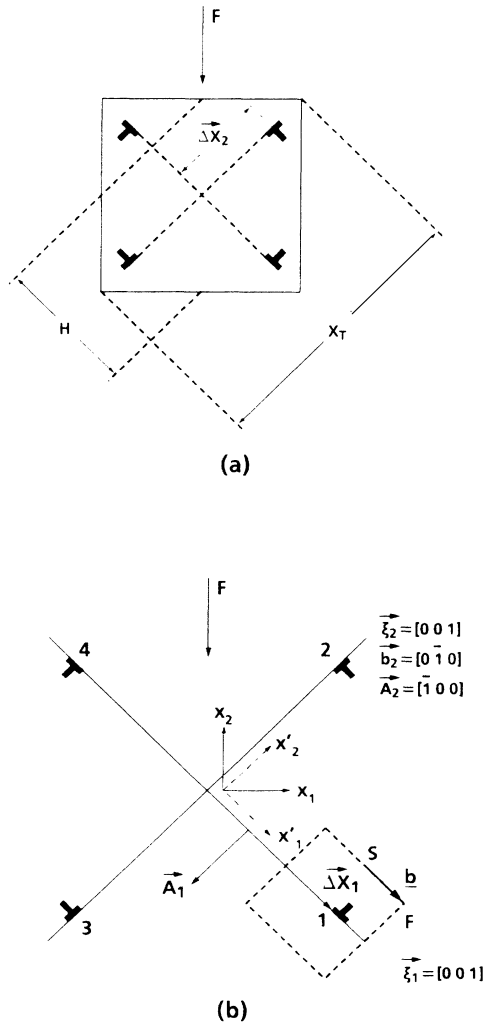

FIG. 3. Shear element (a) model dimensions and (b) strain transformation.

at an arbitrary point with position $\mathbf{r}$ by[8]

$$\mathbf{u}'=[b(\Delta A)/AH](\mathbf{n}\cdot\mathbf{r})\boldsymbol{\beta}\ , \tag{6}$$

where $\mathbf{n}$ is a unit vector normal to the glide plane, $\boldsymbol{\beta}$ is a unit vector in the slip direction, and $\mathbf{A}=(A/b)(\mathbf{b}\times\boldsymbol{\xi})$, with the Burgers vector $\mathbf{b}$ defined according to the SF-RH (start-to-finish, right-hand convention described by Hirth and Lothe[9]) rule specified with respect to the line vector $\boldsymbol{\xi}$. The dislocation line vector and Burgers vector are assigned in a manner consistent with the definition of positive work being done by an external stress. The area swept out by movement of a dislocation line of length l through a distance $\Delta\mathbf{x}$ is given by $\Delta\mathbf{A}=l(\boldsymbol{\xi}\times\Delta\mathbf{x})$ and the shear separation distance $\mathbf{H}$ shown in Fig. 3, is given by $\mathbf{H}=(H/\Delta x)(\boldsymbol{\xi}\times\Delta\mathbf{x})$. By differentiation of Eq. (6), the strain tensor, as described by Bishop[8] and Groves and Kelly[10] for small strain, is obtained,

$$\epsilon_{ij}=\frac{b(\Delta A)}{2HA}(n_j\beta_i+n_i\beta_j)\ . \tag{7}$$

For a slip system oriented as in the case of Fig. 3, this becomes

$$[\epsilon']=\frac{b(\Delta A)}{V}\begin{bmatrix}0 & \frac{1}{2} & 0\\ \frac{1}{2} & 0 & 0\\ 0 & 0 & 0\end{bmatrix}\ . \tag{8}$$

where V is obtained by employing the relationship $\mathbf{A}\cdot\mathbf{H}=V$.

Here we evaluate directly the components of the strain tensor for each of the dislocations of the shear element of Fig. 3 from

$$[\epsilon']_m=\frac{\mathbf{b}_m\cdot(\Delta\mathbf{A}_m\times\boldsymbol{\xi}_m)}{\mathbf{A}_m\cdot\mathbf{H}_m}\begin{bmatrix}0 & \frac{1}{2} & 0\\ \frac{1}{2} & 0 & 0\\ 0 & 0 & 0\end{bmatrix}\ , \tag{9}$$

where m signifies the mth dislocation. Calculation of the strain for the dislocation slip pair $m=1$ and $m=4$ in the (x_1',x_2') system, the nonzero components of the strain in Eq. (9) become

$$(\epsilon'_{12})_{1,4}=(\epsilon'_{21})_{1,4}=\frac{1}{2}\left\{\frac{\mathbf{b}_1\cdot(\Delta\mathbf{A}_1\times\boldsymbol{\xi}_1)}{\mathbf{A}_1\cdot\mathbf{H}_1}+\frac{\mathbf{b}_4\cdot(\Delta\mathbf{A}_4\times\boldsymbol{\xi}_4)}{\mathbf{A}_4\cdot\mathbf{H}_4}\right\}\ , \tag{10}$$

and are evaluated as

$$(\epsilon'_{12})_{1,4}=(\epsilon'_{21})_{1,4}=-\frac{b}{2X_tH}(\Delta x_1+\Delta x_4)\ . \tag{11}$$

Similarly for the dislocation slip pair $m=2$ and $m=3$, the nonzero strain components of Eq. (9) are

$$(\epsilon'_{12})_{2,3}=(\epsilon'_{21})_{2,3}=-\frac{b}{2X_tH}(\Delta x_2+\Delta x_3)\ . \tag{12}$$

The sum of the strain contributions for both slip pairs expressed in the loading coordinate system (x_1,x_2) shown in Fig. 3 results in the dislocation strain state

$$[\epsilon]=\frac{1}{2}\frac{b}{X_t H}\begin{bmatrix} \sum_{i=1}^{m}\Delta x_i & 0 & 0 \\ 0 & -\sum_{i=1}^{m}\Delta x_i & 0 \\ 0 & 0 & 0 \end{bmatrix} . \quad (13)$$

Following the same procedure for the three-dimensional case, where the contributions of the dislocations from two additional 45° planes in a plane section rotated 90° about the 2 axis are included, the strain tensor becomes

$$[\epsilon]=\frac{1}{2}\frac{b}{X_t H}\begin{bmatrix} \sum_{i=1}^{m}\Delta x_i & 0 & 0 \\ 0 & -2\sum_{i=1}^{m}\Delta x_i & 0 \\ 0 & 0 & \sum_{i=1}^{m}\Delta x_i \end{bmatrix} . \quad (14)$$

This shows that the AMS dislocations generated under unidirectional compression produce a three-dimensional state of strain. A similar analysis shows that the Meyers model also produces a nonuniaxial state of strain.[11] The strain tensor above is consistent with the isochoric nature of dislocation movement. The volume change associated with the postreaction dislocation configuration will be evaluated in Sec. V.

IV. MOLECULAR-DYNAMICS SIMULATIONS

Bandak, Tsai, and Armstrong[7] have described, with the method of Tsai,[12] the evolution of a nanoscale dislocation structure from the shock-induced compression of a ten-atom vacancy cluster, as shown in Fig. 2. Primary $\langle 111\rangle$ and related $\langle 100\rangle$ Burgers vector dislocations were produced within a several-layer, forcewise, monatomic body-centered-cubic lattice. A stress-strain description was given for the modeled shock compression. The same method is being applied to evaluation of the stress interaction between sheared dislocations, as is proposed to occur in either the AMS or Smith-Meyers model descriptions.

Figure 4 is shown as an application of the description given here to model results reported by Liu, Zhang, and Yu.[5] In this case, simulation of the shock compression of a two-dimensional "triangular lattice" with atomic interactions following a Lennard-Jones potential was investigated. The dislocation structure obtained by following the present procedures is marked. The two circled dislocation pairs closest to the shock front represent unreacted pairs of the type corresponding to the AMS model. In this latter case, though, the AMS reaction is

$$\frac{a}{2}[\bar{1}01]+\frac{a}{2}[011]=\frac{a}{2}[\bar{1}12] , \quad (15)$$

and is unfavorable on an energy basis, hence, the standoff positions that are shown. Further behind the shock front, the third circle contains a single reacted dislocation in accordance with

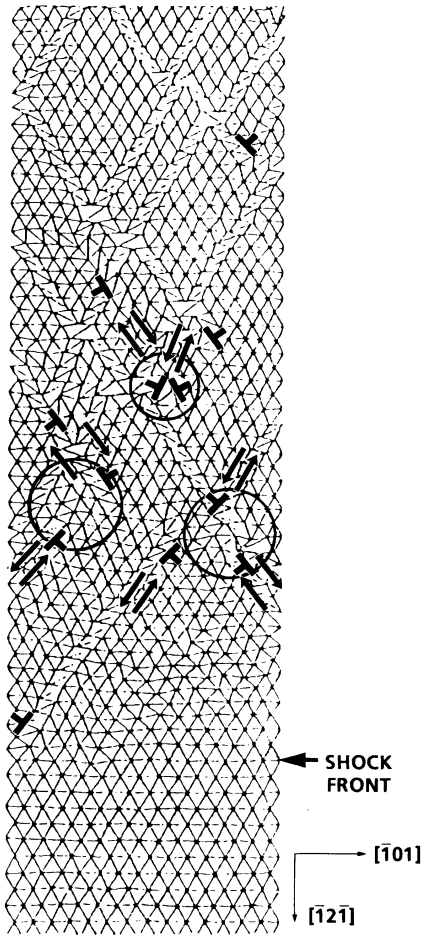

FIG. 4. Dislocation interpretation of Liu, Zhang, and Yu (Ref. 5) shocked "triangular" lattice.

$$\frac{a}{2}[\bar{1}01]+\frac{a}{2}[01\bar{1}]=\frac{a}{2}[\bar{1}10] , \quad (16)$$

and this is consistent with the Smith-Meyers description. This reaction is very favorable, of course, and should be expected to occur in this orientation eventually for all dislocations if sufficient dislocation mobility exists behind the shock front. The application points to the importance of crystal structure and lattice orientation on the shocked dislocation structure.

V. DISLOCATION REACTIONS AND VOLUME CHANGE

The idealized AMS dislocation arrangement was contrived to produce the dislocation reactions shown in Fig. 1(c). The interlocking nature of the proposed shear elements allows reactions to occur and produce the prismatic edge dislocation dipoles. As was shown, the reactant dislocations on 45° planes generate a three-dimensional shape change during their displacement. Only if the dipoles could be imagined to form directly by a fluctuating "punch-type" action, which would produce alternating shear stresses on planes containing the shock propagation

direction, would a fully one-dimensional state of strain result for the dislocated state from start to finish. A schematic of such a process is shown in Fig. 5. This may produce prismatic loops directly with no need for the lateral dislocation motion required to produce reactions. In any case, the residual strain field of the resulting prismatic edge dislocation dipole arrangement produces no volume change in the elastic strain field. This is shown by considering the residual strain field for one dipole embedded in an infinite half space. Following Head's[13] potential theory results which give the stress field of one dislocation at $(x,y)=(a,0)$ in a semi-infinite solid with a free surface at $(0,y)$, the stress field and consequently the strain field of a dipole were calculated. The superposition of strains for the regular arrangement of dipoles gives its full strain field and, therefore, the dipole dilatation is

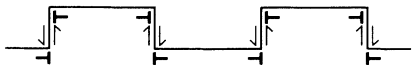

FIG. 5. Direct dipole formation by alternating "punch-type" shear displacements.

$$\delta(x,y)=\epsilon_{xx}(x,y)+\epsilon_{yy}(x,y)+\epsilon_{zz}(x,y)\ , \tag{17}$$

where the strain in the z direction is zero due to the plane strain condition. In terms of stress, the dilatation is

$$\delta(x,y)=\frac{(1+\nu)(1-2\nu)}{E}\{\sigma_{xx}(x,y)+\sigma_{yy}(x,y)\}\ . \tag{18}$$

For dipole dislocations at $(x,y)=(a,h)$ and $(x,y)=(a,-h)$, with orientation giving Burgers vectors perpendicular to the free surface, Eq. (18) becomes

$$\delta(x,y)=\frac{(1+\nu)(1-2\nu)}{E}\{\sigma_{xx}(x-a,y+h)+\sigma_{yy}(x-a,y+h)+\sigma_{xx}(x-a,y-h)+\sigma_{yy}(x-a,y-h)\}\ . \tag{19}$$

After substituting the expressions obtained for the stress components, Eq. (19) becomes

$$\begin{aligned}\delta(x,y)=\frac{(1-2\nu)b}{2\pi(1-\nu)}\Bigg\{&(y+h)\left[\frac{-1}{[(x-a)^2+(y+h)^2]}+\frac{1}{[(x+a)^2+(y+h)^2]}\right.\\&\left.+\frac{4a^2}{[(x+a)^2+(y+h)^2]^2}+\frac{4ax(x+a)^2}{[(x+a)^2+(y+h)^2]^3}\right]\\&+(y-h)\left[\frac{1}{[(x-a)^2+(y-h)^2]}-\frac{1}{[(x+a)^2+(y-h)^2]}\right.\\&\left.-\frac{4a^2}{[(x+a)^2+(y-h)^2]^2}-\frac{4ax(x+a)^2}{[(x+a)^2+(y-h)^2]^3}\right]\Bigg\}\ .\end{aligned} \tag{20}$$

Representing this expression in polar form and integrating gives the volume change for one dipole

$$\Delta V=\int_{-\pi/2}^{\pi/2}\int_{r_0}^{R}\delta(r,\theta)r\,dr\,d\theta\ , \tag{21}$$

where $r_0^2=x_0^2+y_0^2$ is the dislocation cutoff radius and R is the dimension of the crystal. The integral vanishes to verify that no volume change occurs. This result couples with the earlier deformation strain result (from the dislocation movement strain tensor shown above) to produce no net volume change. Both results are consistent with the continuum dislocation theory of plasticity.

VI. DISLOCATION DENSITY AND SHOCK STRENGTHENING

The models discussed, particularly those associated with Meyers and AMS, enable an estimation to be made of the dislocation density values occurring during the shocking process. The high density of dislocations produced by shock loading is proposed to account for the strengthening that has been measured afterwards in a number of materials.[14–17]

On a reasonably direct basis, shock-strengthening measurements may be compared with the often-used relation between dislocation density ρ and flow stress expressed in terms of the resolved shear stress τ

$$\tau=\tau_0+\alpha Gb\sqrt{\rho} \tag{22}$$

where τ_0 is the friction stress for dislocation movement, G is the shear modulus, and α is a proportionality factor. The dislocation density is proportional to the reciprocal value of d^2. Kuhlmann-Wilsdorf[18] has given an updated description of the relationship, including specification of α as

$$\alpha=\frac{(2-\nu)}{12\pi(1-\nu)}\ln\left[\frac{d}{b}\right]\ . \tag{23}$$

Thus, α depends weakly on the cell size d except at small d (i.e., as $d\to b$) where $\alpha\to 0$. This is the region of interest in the present case.

Figure 6 shows the variation of α and $\Delta\tau=\tau-\tau_0$ with cell size d. On this basis, the value of d/b corresponding to a measured total uniaxial strain for nickel under 10 GPa plane shock compression, as considered by Meyers, gives a value of $\alpha=0.240$. Using this value in Eq. (22)

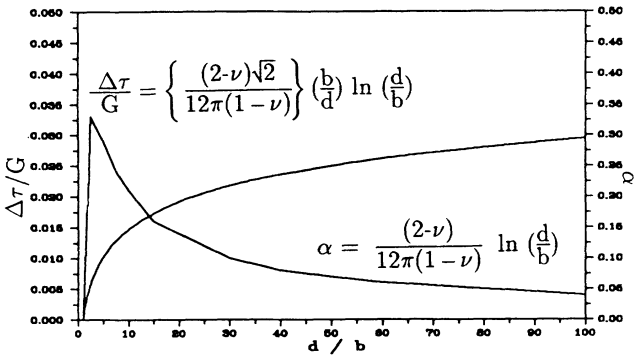

FIG. 6. Kuhlmann-Wilsdorf dislocation parameters for shear-stress–dislocation-density relationship (Ref. 21).

along with the dislocation density reported by Meyers, we find that the predicted strengthening increment is approximately ten times larger than a related experimental result reported by Follansbee and Gray.[19] For the AMS case we reevaluate the value of d/b using Eq. (14), which gives the cell size as

$$d = 4b\sqrt{2}/\epsilon_{22} , \tag{24}$$

recalling here that ϵ_{22} is the component of the dislocation movement strain in the direction of compression. Following Meyers,[2] the strain was calculated at maximum compression volume [see Eq. (1)]. This leads to a 33% lower strain value relative to the total transient strain, including the rarefaction, that was calculated by Follansbee and Gray.[19] Taking the total transient strain into account in the present calculation would reduce the overestimate of strengthening and would bring the results closer to experiment. Applying the present procedure to calculate the dislocation density, the predicted strengthening for the case reported by Follansbee and Gray for nickel, and those reported for pure iron by Dieter,[14] both under 10 GPa shock compression, is still four to five times times greater than the measured values.

Another way to view the strengthening of the postshock prismatic dislocation dipole nanostructure (prescribed by the AMS model) is analogous to that of dislocation loop structures in irradiated iron.[20–23] In both cases the prismatic loops act as obstacles impeding the slip motion of relatively large (in terms of line length) microscale dislocations. Their Burgers vector character presents a reactant feature through which slip dislocations annihilate those components of the dipoles carrying an opposite Burgers sign and intersecting the slip path. This effect, referred to as channeling, is proposed here to be responsible for the observed lack of change in work hardening[24] occurring after the initial strengthening increment in shocked iron and for the indication that the shock strengthening is athermal.[25]

Here, we consider on a more direct basis the shock strengthening of iron where nearly the same experimental results have been reported by the five different sources cited earlier.[14–17,24] We start by considering the strengthening increment resulting from the stress field of the nanostructure prior to any occurrence of channeling reactions. This approach resembles that of the theory of solution hardening.[26] In this case, however, the obstacles are line segments rather than point-source entities. The total stress field of the reacted AMS nanostructure is used to calculate the force acting on a glide dislocation threading through the structure along a particular path. Hardening caused by long-range elastic interaction of dislocations is of interest because of the indicated athermal nature of shock strengthening.

Take a dislocation to be moving parallel on a 45° plane through a two-dimensional cell containing only a pair of dipole dislocations located at the points $(0,h/2)$ and $(0,-h/2)$ as shown in Fig. 7. The dipole dislocations within the cell are assumed to be fixed. With the dislocation line vector taken as $\boldsymbol{\xi}=[100]$ for all dislocations and $\mathbf{b}=[110]$ as the Burgers vector of the slip dislocation, the added glide force becomes

$$F_g(x,y\pm h/2)=b[\sigma_{22}(x,y\pm h/2)-\sigma_{11}(x,y\pm h/2)] , \tag{25}$$

where σ_{22} and σ_{11} are the dipole stress components evaluated at the position of the slip dislocation. Substitution of these stresses gives the glide resistance force due to one dipole

$$F_g(x,y\pm h/2)=\frac{Gb^2x}{\pi(1-\nu)}\left\{\frac{2(y+h/2)^2}{[x^2+(y+h/2)^2]^2}+\frac{(y-h/2)^2}{[x^2+(y-h/2)^2]^2}\right\} , \tag{26}$$

where h is equal to half the dipole separation d. A summation of the contributions of all the dipoles gives the force on a dislocation moving through the AMS nanostructure. The general case, where nanoscale dislocations may occur and react to form a less uniform distribution of dipoles, still retains the dislocation spacing and sign distribution as the determining features for the resistance to glide.

A 12-dislocation cell was found to be representative of

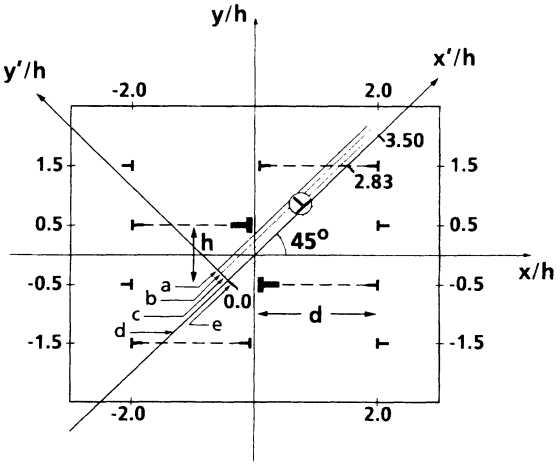

FIG. 7. Glide paths for force calculations on a dislocation threading through the AMS nanostructure.

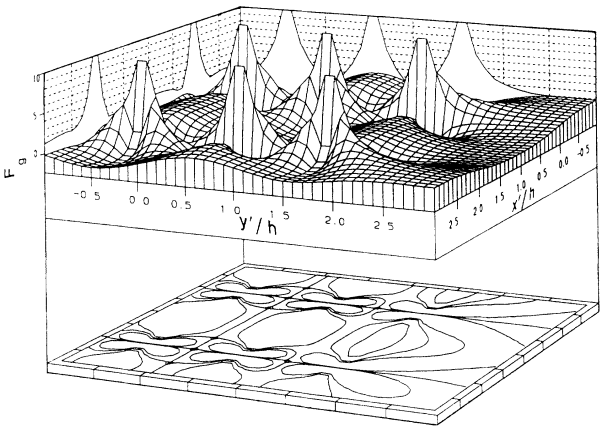

FIG. 8. Position dependence of the glide dislocation force F_g in units of $Gb^2/\pi(1-\nu)h$.

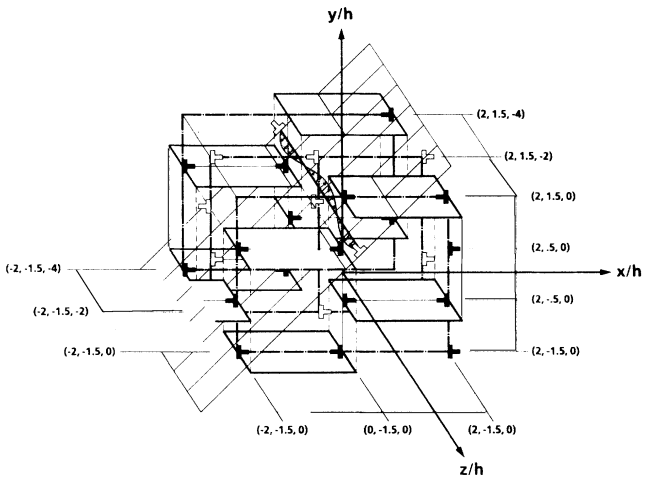

FIG. 10. Postshock glide dislocation threading through the shock-generated nanostructure.

the periodic AMS distribution of dislocations and was used to estimate the glide force. Figure 8 shows the variation of the force acting on a dislocation attempting to pass through the cell along any 45° plane, thus giving the obstacle strength it will encounter as it passes along each of the possible paths, through the AMS dislocation array. The force along selected paths of interest is plotted in Fig. 9. The path of least resistance corresponds to path *d* in Fig. 7 and is the one passing through the dipole cell midpoint. Evaluation of the total work required to move the dislocation through the varying force represented by curve *d* in Fig. 9 for the AMS cell leads to an average stress increase of $(0.136)Gb/h$. This value represents a strengthening increment that is approximately twice that experimentally measured for nickel and iron at 10 GPa as referenced earlier. We suggest that this overestimate results because of the presumption of a constant resistance to movement all along the dislocation line. For example, at the maximum force position along path *d*, the dislocation line segment between adjacent cells in Fig. 10 would actually experience zero force itself on the basis of a two-dimensional calculation, thus the average force on the two-dislocation line segments would be reduced roughly by a factor of 2. A formulation accounting for this consideration of a variable force acting along the line length of the threading dislocation is being investigated, along with the additional consideration of dislocation interactions for the three-dimensional AMS structure.

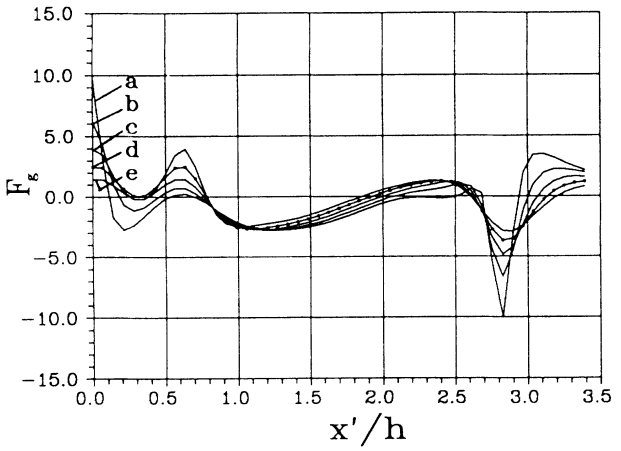

FIG. 9. Force F_g in units of $Gb^2/\pi(1-\nu)h$ vs x'/h (see Fig. 7).

VII. SUMMARY

The achievement of strain uniaxiality within a plane shock profile using several dislocation models was studied. In particular, the stress and strain states of the Armstrong, Miller, and Sandusky (AMS) model were calculated, and the proposed scheme by which dislocations might be generated under shock compression was evaluated. The results show that the Smith-Meyers model produces a nonuniaxial state of strain under assumed one-dimensional plane shock wave compression conditions. They also show that, although the AMS model does not produce uniaxial strain throughout, it does produce a residual state of essentially uniaxial strain. This is due to the proposed reactant dislocations being in the form of dipole pairs consisting of alternating sign Burgers vectors oriented parallel and antiparallel to the shock wave propagation direction. The AMS process is shown to be volume conserving.

Some evidence from the molecular-dynamics results of Liu, Zhang, and Yu is obtained for the validity of the dislocation models, particularly for the AMS version. The resulting prismatic loop configuration was viewed in a similar way to that observed in irradiated crystalline solids and was used to estimate the extent of material strengthening. Calculation of the strengthening increment using an accepted relation between the resolved shear stress and dislocation density led to higher values than those measured. A calculation based on an obstacle distribution approach similar to that of Nabarro's theory of solution hardening with dislocation dipoles in this case gave closer, though still higher stresses than those measured. We attribute the discrepancy to the presumed resistance to movement of a straight dislocation line,

whereas the idealized three-dimensional AMS network presents attractive as well as repulsive forces acting on the dislocation line segments.

ACKNOWLEDGMENTS

One of the authors (F.A.B.) thanks Dr. M. Moussouros for valuable discussions. Thanks are also extended to Mr. D. E. Phillips, Mr. K. W. Reed, Mr. R. A. Kavetsky, and Mr. W. W. McDonald of the Naval Surface Warfare Center for their encouragement of this work. The work of one of us (F.A.B.) was performed with support from the NSWC White Oak Laboratory. The work of another (R.W.A.) was supported by ONR Contract No. N00014-86-K-0286.

[1]C. S. Smith, Trans. TMS-AIME **212**, 574 (1958).
[2]M. A. Meyers, Scr. Metall. **12**, 21 (1978).
[3]R. W. Armstrong, R. S. Miller, and H. W. Sandusky, in *ONR Workshop on Dynamic Deformation, Fracture, and Transient Combustion* (Chemical Propulsion Information Agency Publication **474**, Chestertown, MD, 1987), p. 77.
[4]J. N. Johnson, Appl. Phys. Lett. **50**(1), 28 (1987).
[5]G. Liu, R. Zhang, and W. Yu, J. Phys. (Paris) Colloq. **49**, C3-387 (1988).
[6]M. A. Mogilevsky, J. Phys. (Paris) Colloq. **49**, C3-467 (1988).
[7]F. A. Bandak, D. H. Tsai, and R. W. Armstrong, in *Shock-Wave and High-Strain-Rate Phenomena in Materials,* edited by M. A. Meyers, L. E. Murr, and K. P. Staudhammer (Marcel Dekker, New York, 1992), Chap. 89, p. 957.
[8]J. F. Bishop, Philos. Mag. **44**, 51 (1953).
[9]J. P. Hirth and J. Lothe, *Theory of Dislocations* (Wiley, New York, 1982), p. 21.
[10]G. W. Groves and A. Kelly, Philos. Mag. **8**(89), 877 (1963).
[11]F. A. Bandak, A. S. Douglas, R. W. Armstrong, and D. H. Tsai, in *Proceedings of the Second International Symposium on Plasticity and Its Applications* (Mie University, Tsu Japan, 1989).
[12]D. H. Tsai, in *Chemistry and Physics of Molecular Processes in Energetic Materials,* Vol. 307 of NATO Advanced Study Institute, edited by S. N. Bulusu (Kluwer Academic, Norwell, MA, 1990), pp. 195-227.
[13]A. K. Head, Proc. Phys. Soc. London, **B66**, 793 (1953).
[14]G. E. Dieter, in *Response of Metals to High Velocity Deformation,* edited by P. G. Shewmon and V. F. Zackay (Interscience, New York, 1961), p. 409.
[15]E. G. Zukas and C. M. Fowler, in *Response of Metals to High Velocity Deformation* (Ref. 14), p. 343.
[16]T. Arvidsson, and L. Eriksson, in, *Metallurgical Effects at High Strain Rates,* edited by R. W. Rohde, B. M. Butcher, J. R. Holland, and C. H. Karnes (Plenum, New York, 1973), p. 605.
[17]B. G. Koepke, R. P. Jewett, and W. Chandler, Trans. Am. Soc. Met. **58**, 510 (1965).
[18]D. Kuhlmann-Wilsdorf, Mater. Sci. Eng. **A113**, 1 (1989).
[19]P. S. Follansbee and G. T. Gray, in *Advances in Plasticity 1989,* edited by A. Khan and M. Tokuda (Pergamon, New York, 1989), p. 385.
[20]B. L. Eyre, Philos. Mag. **7**, 2107 (1962).
[21]B. L. Eyre and R. Bullough, Philos. Mag. **12**, 31 (1965).
[22]B. C. Masters, Philos. Mag. **11**, 881 (1965).
[23]B. L. Eyre and A. F. Bartlett, Philos. Mag. **12**, 261 (1965).
[24]B. D. Goldthorpe, T. D. Andrews, and M. C. Hogwood (unpublished).
[25]R. W. Armstrong (unpublished).
[26]F. R. N. Nabarro, Philos. Mag. **35**, 613 (1977).

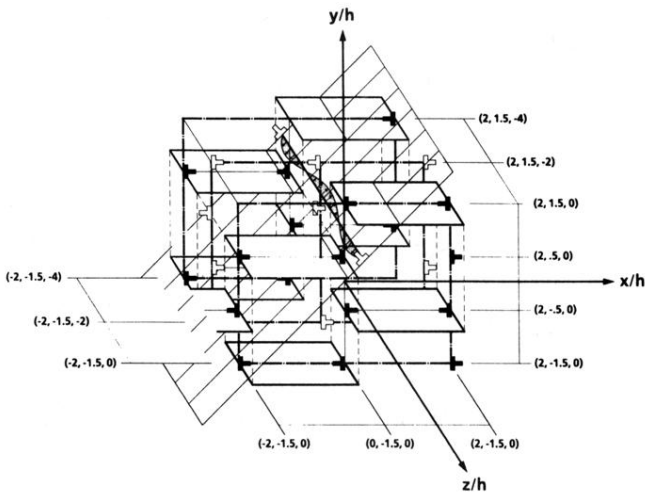

FIG. 10. Postshock glide dislocation threading through the shock-generated nanostructure.